

# Formation of pure anatase $\text{TiO}_2$ by reactive pulsed dc magnetron sputtering: method for controlling target poisoning state

Nikolai Desch<sup>1</sup> and Markus Lake<sup>1</sup>

<sup>1</sup>Hochschule Niederrhein - Campus Krefeld Sud

March 22, 2023

## Abstract

The use of pulsed dc-sputtering sources for reactive magnetron sputtering with oxygen offers a possibility to suppress the negative effects of target poisoning (such as arcing). This results in a wide process range for the selection of a desired operating point. The control of target poisoning plays a major role in maintaining constant coating properties and affects the stoichiometry of the reactive coating, as well as the coating rate and the economic impact of the coating process. In a hysteresis, the target poisoning during the reactive sputtering of titanium under oxygen addition proceeds nonlinearly. Without the use of a suitable target poisoning control technique, the sputtering process can abruptly change to an unstable state. As a result, variations of stoichiometry can occur during the deposition process. A proven method for maintaining a stable reactive sputtering process is the control of oxygen flow with the input variable target voltage. By determining the typical oxygen hysteresis at constant target power and constant argon flow, an operating point for the control loop is derived. The desired target voltage then serves as the input variable for the control loop of the target poisoning. The controlling technique for target poisoning is a basic requirement for the production of the photocatalytic active anatase phase of titanium dioxide ( $\text{TiO}_2$ ) using reactive magnetron sputtering. The photocatalytic equipment of surfaces with a titanium dioxide coating in the anatase phase can be realized with the reactive pulsed dc magnetron sputter ion plating process (DC-MSIP). The pulsed DC-MSIP process facilitates coating a variety of surfaces at temperatures below 200 °C in an environmentally friendly manner.

Nikolai Desch ORCID iD: 0000-0002-0384-8248

Markus Lake ORCID iD: 0000-0002-3535-8454

Formation of pure anatase  $\text{TiO}_2$  by reactive pulsed dc magnetron sputtering

Method for controlling target poisoning state

Nikolai Desch<sup>1\*</sup>, Markus Lake<sup>1</sup>

<sup>1</sup> Hochschule Niederrhein, Reinarzstraße 49, 47805 Krefeld, Germany

\*corresponding author: + 49 2151 822-5086 | [nikolai.desch@hs-niederrhein.de](mailto:nikolai.desch@hs-niederrhein.de)

**Keywords:** reactive sputtering, dc magnetron sputtering (DC-MSIP), pulsed magnetron sputtering (PMS), oxygen, target poisoning, magnetron sputter ion plating,  $\text{TiO}_2$ , anatase

## Abstract

The use of pulsed dc-sputtering sources for reactive magnetron sputtering with oxygen offers a possibility to suppress negative effects of target poisoning (such as arcing). This results in a wide process range for the selection of a desired operating point. The control of target poisoning plays a major role in maintaining

constant coating properties and affects the stoichiometry of the reactive coating, as well as the coating rate and the economic impact of the coating process. The target poisoning during the reactive sputtering of titanium under oxygen addition proceeds nonlinear in a hysteresis. Without the use of a suited target poisoning control technique the sputtering process can abruptly change to an unstable state. As a result, variations of the stoichiometry can occur during the deposition process. A proven method for maintaining a stable reactive sputtering process is the control of oxygen flow with the input variable target voltage. By determining the typical oxygen hysteresis at constant target power and constant argon flow, an operating point for the control loop is determined. The desired target voltage then serves as the input variable for the control loop of the target poisoning. The controlling technique for target poisoning is a basic requirement for the production of the photocatalytic active anatase phase of titanium dioxide by means of reactive magnetron sputtering. The photocatalytic equipment of surfaces with a titanium dioxide coating in the anatase phase can be realized with the reactive pulsed dc magnetron sputter ion plating process (MSIP). The pulsed dc MSIP process provides the ability to coat a variety of surfaces at temperatures below 200 °C in an environmentally friendly manner.

## 1. Introduction

Surface technology describes the summary of a large variety of processes that are used when conventional materials no longer meet increasing demands for wear, corrosion or special tribological or optical requirements. The overall function of a component is therefore often divided into subfunctions. In this case, the surface coating takes a specific function and thus enables the selection of a less expensive base material while at the same time fulfilling the range of requirements for the entire component. Today's application areas of surface technology extend far beyond the function of producing decorative, tribological or corrosion-protective surface coatings. Surface engineering processes are nowadays already an integral part of production and manufacturing, and are often the driving force behind the implementation of product requirements. Furthermore, economic aspects play an important role for the use of coating processes. [1]

All surfaces that we come into contact in our everyday activities have a special role in spreading pathogens. Especially high traffic touched surfaces in public transport or health care can be affected unnoticed. Titanium dioxide is photocatalytically active in its anatase phase and can therefore be used as a self-cleaning, antimicrobial surface coating system. Particularly with regard to the formation and spread of bacteria (e.g. coli bacteria), germs (e.g. MRSA), fungi and algae, anatase can assist in minimizing their formation and spread. In healthcare, follow-up diseases caused by contact with germs, bacteria or viruses are one of the most frequent causes of death worldwide [2]. The so-called multi-resistant germs (MRSA) represent a further problem. In the European economic area, more than 670,000 infections and 33,110 deaths could be attributed to antibiotic-resistant germs during 2015. The total number of infections has increased in the period from 2007 to 2015. Approximately 64 % of all cases in this period occurred due to infections in relation to health care facilities. At least half of the infections are considered to be preventable [3]. All surfaces that patients come into contact with during their stays in a healthcare facility have a major impact on the spread of infections and diseases. A common door handle used by patients and visitors can thus become a critical transmission surface for bacteria and germs. In the analysis of statistical data examining infections for their cause, it was determined that in 21.1 % of the cases the reason was the contact with contaminated medical equipment and in 19.8 % of the cases contamination of the environment was responsible for an infection [4]. The photocatalytic activity of titanium dioxide is based on the release of radicals on the surface which can decompose organic substances in an advanced oxidation process (AOP). The photocatalytically active surface coating offers a physical effect that is able to decompose organic deposits upon irradiation with ultraviolet light. The UV light exposure initiates an advanced oxidation process of the organic substances [5]. A potential formation of a biofilm and a possible risk of infection is thereby reduced and in the best case completely prevented [6]. Further applications of titanium dioxide can be found in the treatment of wastewater with pharmaceutically contaminated residues. [5, 7]

## 2 Magnetron Sputter Ion Plating (MSIP)

Since the first development of an apparatus for sputtering solids by bombarding particles in a vacuum by Penning in 1936, numerous technological developments and research efforts have driven magnetron sputtering as a coating technology. Approximately 50 years ago, the development of sputtering technology progressed greatly and was characterized by successes in improving deposition rates, process stability, and cost efficiency in the following years. At present, magnetron sputtering is widely known as a reliable and cost-effective coating process that has already become established in numerous industries [8]. The MSIP-PVD process is also known as cathode sputtering and can be used for the deposition of metallic coatings (e.g., Ti, Al, Cr), nitride coatings (e.g., CrAlN, TiAlN, TiN, CrN), or oxide ceramic coatings (e.g., Al<sub>2</sub>O<sub>3</sub>, Cr<sub>2</sub>O<sub>3</sub>). The coating can also be produced in several layers, in so-called multilayer coatings. The base material for the deposition of a coating is called the target and is fixed onto a target carrier in the deposition source, the magnetron. Here, the target can be a pure solid material or it can be bonded to a copper backing plate. Bonded targets are often preferred when the target material is expensive and, depending on the target material, it can be necessary to use a backing plate, for instance, if the material is brittle. In the magnetron, magnets, cooling, and a current feed-through to the target are present behind the target. The target is also called the cathode because it is connected to the negative pole of the power supply, whereby it is electrically isolated from the rest of the magnetron. The anode of the magnetron is frequently connected to the coating chamber as a reference potential and the combination of a magnetron source with a power supply defines the particular sputtering process. The selection of different power sources for cathode sputtering allows for a large number of different process variations. Proven processes in practice are direct current magnetron sputtering (DCMS), pulsed magnetron sputtering (PMS), and pulsed high current magnetron sputtering (HIPIMS). The DCMS process is well-suited for sputtering metallic target materials. However, by choosing the PMS method with a power source that can be operated with a pulse mode in the range of medium frequencies (e.g., 100 kHz to 350 kHz), even nonconductive target materials (e.g., Al<sub>2</sub>O<sub>3</sub> or SiO<sub>2</sub>) can be sputtered [9]. The unipolar or bipolar pulsed operation of magnetron sputtering power supplies offers a wide range of variations in parameters by changing the pulse frequency and pulse duty cycle. With regard to the development of new coating processes or the optimization of existing coating systems, this results in a wide range of potential.

### 2.1 Reactive pulsed DC-MSIP

Sputtering of pure metallic coatings usually takes place using argon as an inert process gas. In this process, the inert argon atoms pass through the process of ionization and recombination with electrons several times and are thus frequently reused before they are captured by the vacuum pumping unit. If a reactive gas, such as oxygen or nitrogen, is also introduced, it chemically combines with the target plasma and forms an oxide in the case of oxygen or a nitride in the case of nitrogen. For homogeneous reactive layer formation, a uniform and controllable supply of the reactive gas is essential. The reactive gas is introduced in close range to the target. Usually, tubes with small holes are placed along the target for a homogeneous supply of the process and reactive gases. Similarly to inert gas, the reactive gas becomes ionized and is accelerated onto the target. Therefore, adding to the reaction with the target plasma also helps to contribute to the sputtering process. Since the reactive gas can also be ionized, it is possible to sputter without inert process gas in a pure reactive gas atmosphere. However, this method is rarely used in practice, and generally, a constant flow is maintained with the process gas while the reactive gas is added in a pressure-controlled manner. The control of the reactive gas via the partial pressure can be used as a manipulated variable for the stoichiometry of the layer formation [10, 11].

Three main processes are involved in a reactive deposition, whereby the main process of deposition is sputtering on the target surface. Simultaneously, when reactive gas is introduced into the deposition chamber, getter processes occur on the target surface, the substrate surface, and the chamber walls of the deposition

equipment. Getter processes occur when layers are formed by the interaction of reactive gas atoms and they take place in various forms on all surfaces in a coating system. Getter processes that take place on the target surface are also known as “target poisoning.” As the supply increases, the reaction with reactant gas causes the sputtering yield to decrease because of the increasing occupancy of the target. The secondary electron yield thus increases and the plasma impedance decreases, resulting in a reduced cathode voltage at the magnetron. The sum of the events leads to a hysteresis behavior in the process of reactive magnetron sputtering. While the stoichiometry in the deposition of nitrides can generally be relatively easily controlled via the partial pressure of the reactive gas, the process of target poisoning in the reactive sputtering of oxides behaves much more dynamically and is therefore more difficult to control with conventional DC-MSIP. As the target surface is also covered by an oxide layer during the deposition process, the resulting lower electrical conductivity of the oxide layer leads to increased arcing, which in turn results in an extremely unstable sputtering process, creating undesired droplets of molten target material, and can even destroy the sputtering target. The use of a pulsed DC source for magnetron sputtering can overcome these disadvantages as the pulsed mode of the magnetron with frequencies ranging from 100 kHz to 350 kHz avoids arcing on the target surface, since it is covered with an oxide layer.

### 3. Experimental Design and Results

The Raman analysis of the coatings was performed with a Renishaw InVia Raman spectroscope, and a green laser with a wavelength of 532 nm and a laser power of 0.75 mW was used. All titanium dioxide coatings were produced on the Metaplas Domino.Mini industrial PVD coating system. In this work, pulsed DC-MSIP is the applied coating technology. The titanium target used has a size of 456 mm x 81 mm x 10 mm and is made of 99.999 % pure titanium. A sputtering power of 7.0 kW was applied for all experiments, which corresponds to a power density of approximately 19 W/cm<sup>2</sup>. Argon with a purity of 99.999 % was used as the process gas. The reactive gas oxygen has a purity of 99.998 %. Conventional slides were used as substrate material (soda-lime float glass slides 76 mm x 26 mm x 1.5 mm) and the maximum substrate temperature was recorded using a drag gauge thermometer. The magnetic field strength perpendicular to the target was 24.9 mT. For the coating experiment, the glass slides were ultrasonically cleaned in technical ethanol (96 %) for 10 minutes and the cleaned slides were subsequently charged on the substrate table. After loading the coating chamber, the chamber was evacuated to a starting vacuum of 4.0 x 10<sup>-3</sup> Pa. Afterwards, without additional heating, an argon-ion sputter etching was performed for 15 minutes. Following the etching process, the coating process was carried out using the reactive pulsed magnetron sputtering method, also without additional heating. The turbomolecular pump (Turbovac Mag W 1600 iP) was kept constant at 25,200 rpm during the coating experiment. All coating experiments were operated in power-constant mode with 7.0 kW dc pulsed sputtering power. For all experiments, the applied pulse parameters were kept constant. Figure 1 shows the voltage (a) and current (b) curves during the PMS process, recorded with a Tektronix TDS 2001C oscilloscope, measured at the Advanced Energy Pinnacle Plus+ power source on the Metaplas Domino.Mini coating system. The applied pulse frequency was 350 kHz with a switch-on time ( $t_{on}$ ) of 1.7  $\mu$ s and the switch-off ( $t_{off}$ ) in this case was 1.1  $\mu$ s. The pulse duration T was 2.8  $\mu$ s. The switch-on time corresponds to a 60 % duty cycle ( $t_{on} / t_{on} + t_{off}$ ). Further detailed explanations of the pulsed dc mode can be found in [12–14].

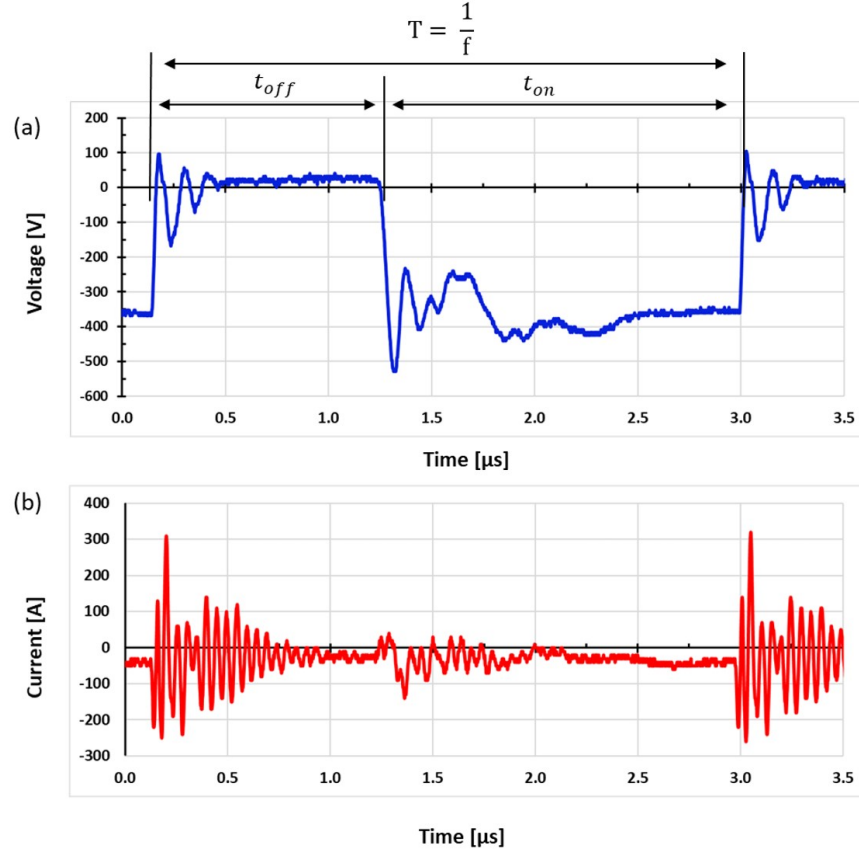


**Figure 1:** Voltage (a) and current (b) charts of the reactive pulsed dc magnetron sputtering process, 350 kHz pulse frequency, 7 kW constant power mode, 60 % duty cycle

### 3.1 Hysteresis tests for the determination of target poisoning state

In the common DCMS, a reactive sputtering process of an oxide layer results in an electrical charging of the magnetron and thus leads to arcing. The PMS method pulses the sputtering power and in the off times, a charge of the magnetron can discharge again. The pulsed operation of the magnetron enables a consistent stable deposition process for oxide films. Figure 2 shows the magnetron voltage recorded during the pulsed magnetron sputtering process at a constant argon flow of 120.0 sccm. The addition of oxygen was linearly varied in each case over a five-minute period. In this case, the sputter power was 7.0 kW with a dc pulsed mode at 350 kHz and a switch-on time of 1.7  $\mu\text{s}$ . The hysteresis behavior of the reactive sputtering process of titanium dioxide can be used to explain the effect of target poisoning. Figure 2 shows six states of target poisoning from a) to f) on a schematic cross-section of a target with the typical sputtering erosion.

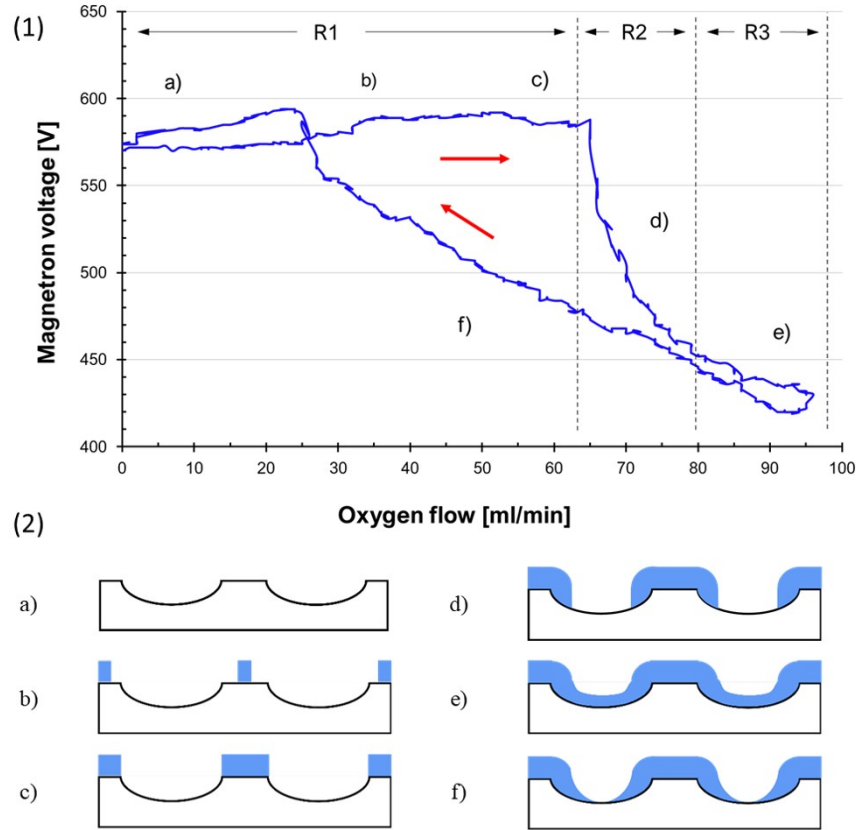


**Figure 2:** (1) Magnetron voltage during the reactive pulsed dc magnetron sputtering process with target poisoning regions (R1-R3) and (2) schematic illustration of target poisoning state

The states of the target poisoning were assigned to the respective areas in the upper graph in Figure 2 which represents the progression of magnetron voltage over the linear increase in oxygen flow from 0 sccm to 96 sccm which was followed by a direct linear decrease in oxygen flow to 0 sccm. Recording a hysteresis plot during magnetron sputtering is an important step in detecting sputtering regions and the target poisoning state. In a hysteresis experiment, all settings are kept constant except for the variation of the reactive gas flow. At the beginning of the hysteresis experiment, the metallic sputtering region was present (approximately up to 30 sccm), since no target poisoning had occurred (a in Figure 2). As the oxygen flow increased, the target surface poisoning commenced outside the sputtering erosion (b in Figure 2). The target poisoning increased from 30 sccm to approximately 60 sccm oxygen flow to the point where the target surface was completely poisoned except for the sputtering erosion (c in Figure 2). The high ion density in this region provides enhanced sputtering in these areas of the target and is also responsible for keeping the sputtering erosion clear until shortly before the transition region (Region 2 in Figure 2). The magnetron voltage is very constant in the metallic region and only shows a small increase of approximately 20 V. Just past a slight increase in oxygen flow, in the metallic region at about 60 sccm oxygen flow, the process shifted to the unstable transition region (Region 2 in Figure 2). The transition region was characterized by an increase in target poisoning until partial saturation of the sputtering erosion (d in Figure 2). A relatively small increase of 15 sccm from 65 sccm oxygen flux to 80 sccm caused a rapid decrease in the magnetron voltage from 590 V to 450 V. In the transition area, the magnetron voltage displayed a rapid change over to the completely poisoned area. A small increase in oxygen flow of 10 sccm caused a sharp decline in magnetron voltage of 140 V and positioned the sputtering process to shift into the fully poisoned sputtering area. A further increase

of the oxygen flow above 90 sccm only caused a slight decrease in the magnetron voltage but led to the complete poisoning of the target surface (e in Figure 2). Once the state of full poisoning was reached at 96 sccm, the flow was decreased to the starting value for the same duration. Based on the magnetron voltage plot, as the oxygen flow decreased, it became evident that the target poisoning was not behaving similarly to the increase of oxygen flow. The steep decrease in the transition region was not reversed to the same extent during the decrease in the oxygen flow. The total target poisoning only weakly decreased over a relatively large decrease from 70 sccm to approximately 25 sccm (f in Figure 2). If complete target poisoning occurs, the target is only atomized slowly due to the complete occupancy of titanium dioxide with the same decrease in oxygen flow, whereby the relatively slow atomization compared to the initially metallic region is the main influence. Since the target was completely covered with oxide and oxygen was constantly supplied, the sputtering process only reached the metallic sputtering region directly after a large decrease in oxygen flow. Since the magnetron voltage is a value that can directly be measured and the flux control is a manipulated value, both values can be used for a control loop to control the sputtering region of the reactive deposition. Usually, a magnetron voltage from the transition range, e.g. 500 V, is selected as desired value, and in a regulating concept of this kind, the oxygen flow is then adjusted to the desired magnetron voltage. Such a feedback system is used on the PVD coating system Metaplas Domino.Mini, at the Niederrhein University of Applied Sciences, for the sputtering of oxides. Since hysteresis in reactive magnetron sputtering is always system dependent and influenced by the respective systems and plant conditions, the measurement of the hysteresis behavior is important for the investigation of an efficient and stoichiometric operating set point for the deposition of oxides.

The coating process, consisting of the generation of a bonding layer and the functional layer, was carried out in four consecutive phases. First, the magnetron was ramped up for three minutes at a constant argon flow of 120 sccm in front of a shading plate. During start-up, the sputter power was ramped up in two minutes from 0.5 kW to 7.0 kW followed by a ramp-down from 7.0 kW to 2.0 kW in one minute. During this process, the target surface was cleaned of any oxide layers. In the second phase, the shading plate was moved away from the magnetron and a pure titanium layer was deposited on the substrate for three minutes. The shading plate was subsequently moved back in front of the magnetron. In the third phase, the sputtering power was again increased to 7.0 kW. As soon as the sputtering power of 7.0 kW was reached, the oxygen control circuit was activated with the desired magnetron voltage. For a period of three minutes, the shading plate continued to be coated. During the fourth phase, the shading plate was moved away from the magnetron and the reactive coating process with titanium dioxide was carried out for five hours. The coating phase was followed by a one-hour cooling phase. All coating experiments were conducted with the same etching process, and with no additional heating and no BIAS during the coating process. The process gas flow was changed in three stages starting at 120 sccm, subsequently moving to 160 sccm, and finally up to 200 sccm. For each process gas flow, three operating points out of the transit region of target poisoning were chosen (Region 2 in Figure 2). The hysteresis behavior was generally divided into two stable sputtering areas, namely metallic (Region 1 in Figure 2) and reactive (Region 3 in Figure 2). An unstable transition area (Region 2 in Figure 2) was observed between the two stable areas. Although the metallic mode of operation has the advantage of high deposition rates, reactively deposited films from this region are substoichiometric. In the reactive sputtering region, the deposited layers are ideally stoichiometric with the disadvantage that the deposition rates are a factor of 5 to 10 times smaller than in the metallic sputtering region. The hysteresis behavior is prominent in the sputtering of oxide layers, e.g.  $\text{Al}_2\text{O}_3$  or  $\text{TiO}_2$ , and the process window for an economical and stoichiometric deposition is located in the transition area between the reactive and metallic sputtering areas. The sputtering behavior in the transition region poses unique challenges for process control since a relatively small change in the gas regulation of oxygen can lead to strong change target poisoning [15].

## 3.2 Experimental design

For the synthesis of the anatase titanium dioxide modification, the relevant literature was reviewed. Based on the findings, the absolute process pressure proved to be an important process parameter whereas it was concluded that additional heating and application of BIAS voltage were not important to improve the formation of the anatase phase. Table 1 presents an overview of successfully prepared anatase phases from various publications.

**Table 1:** Comparison of PVD process parameters for the deposition of anatase titanium dioxide

Sputter Process	Pressure [Pa]	Oxygen ratio in Argon/Oxygen-Mix [%]	Reference
DC	1.0	20	[10]
	1.0	30	[26]
	$2.7 \times 10^{-1}$	100	[27]
	$2.7 \times 10^{-1}$	16.6	[28]
	$7.0 \times 10^{-1}$	30	[29]
	$7.0 \times 10^{-1}$	14.6	[27]
pulsed DC	4.0	34.4	[16]
	$4.0 \times 10^{-1}$	30	[30]
	1.5	30	[17]
	$6.0 \times 10^{-1}$	20	[31]

To ensure that this range can be achieved during reactive pulsed magnetron sputtering on the present coating system, the process pressure is initially determined at different process gas settings and constant reactive gas flow (Table 2). The supply of argon and oxygen combined with the power control of the vacuum pumping system affects the final chamber pressure. For a first rough selection, an extra oxygen addition of 70 ml/min has been chosen. This acted as an initial guess for the choice of argon flow. In the real sputtering process, deviations are to be expected due to getter processes of the titanium atomization and the subsequently selected operating point. Table 2 shows the results of this experiment at constant addition of 70 ml/min oxygen and under variation of the argon flow. Here, the pure process pressure was recorded without the sputtering process being in progress. The turbomolecular pump was kept at a constant 60 % power. The argon flow was varied from 100 ml/min in 20 ml/min steps up to a maximum of 240 ml/min. Possible deviations in the real process were accepted at this point and the determination at this point was only used to generate suitable changes in the process pressure via the control of the argon flow. As an approach, the real experiments will proceed from lower range of process pressure to higher range process pressure.

**Table 2:** Determination of the absolute process pressure

Argon flow [ml/min]	Process pressure [Pa]	Process pressure with addition of 70 sccm Oxygen flow [Pa]
100	$3.7 \times 10^{-1}$	$0.65 \times 10^{-1}$
1200	$4.4 \times 10^{-1}$	$0.75 \times 10^{-1}$
140	$5.3 \times 10^{-1}$	$9.3 \times 10^{-1}$
160	$6.3 \times 10^{-1}$	1.1
180	$7.2 \times 10^{-1}$	1.5
200	$8.4 \times 10^{-1}$	2.1
220	1.0	2.8
240	1.4	3.2

Possible deviations in the real process were accepted at this point and the determination was only used to generate suitable changes in the process pressure via the control of the argon flow, whereas the actual

experiments proceeded from a lower range of process pressure to a higher range process pressure. In a real sputtering process, deviations are to be expected due to target poisoning, getter processes, and the chosen operating point, which means that the chamber pressure will be slightly lower or higher than predicted, depending on the choice of the operating point. The values of 120 sccm, 160 sccm, and 200 sccm were selected as suitable process gas settings and the investigation of the hysteresis behavior at the three predefined process gas settings commenced. As described in Chapter 3.1 in Figure 2, three hysteresis courses of the target poisoning were recorded using this procedure of hysteresis determination. Figures 3, Figure 4, and Figure 5 portray the determination of working points from three hysteresis experiments, whereby the choice of the working points in each case was made from the transition area of the target poisoning. All three experiments were determined at a constant target power of 7.0 kW. The hysteresis of Figure 3 was determined at a constant argon flow of 120 sccm, while that in Figure 4 was measured at 160 sccm and Figure 5 at 200 sccm. Three operating points were selected from each of the three hysteresis patterns, resulting in a total of nine experimental settings.

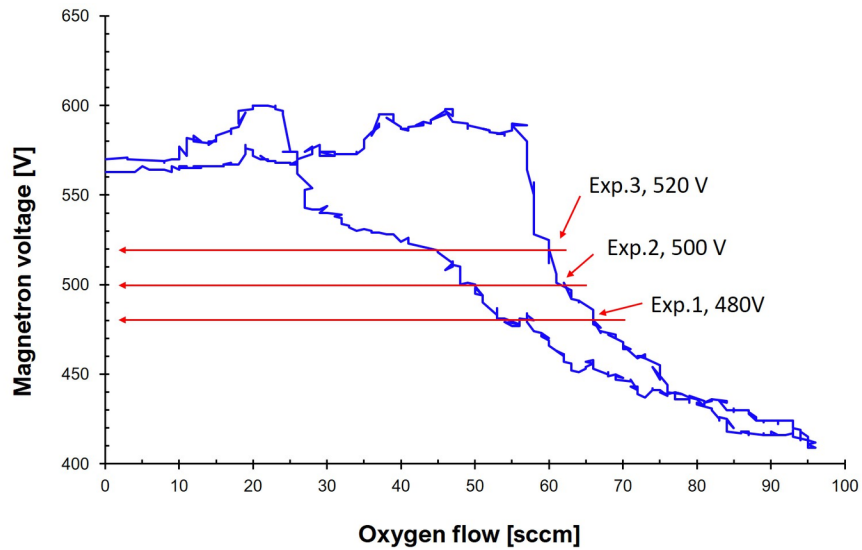


**Figure 3:** Hysteresis characteristics at constant argon flow 120 ml/min

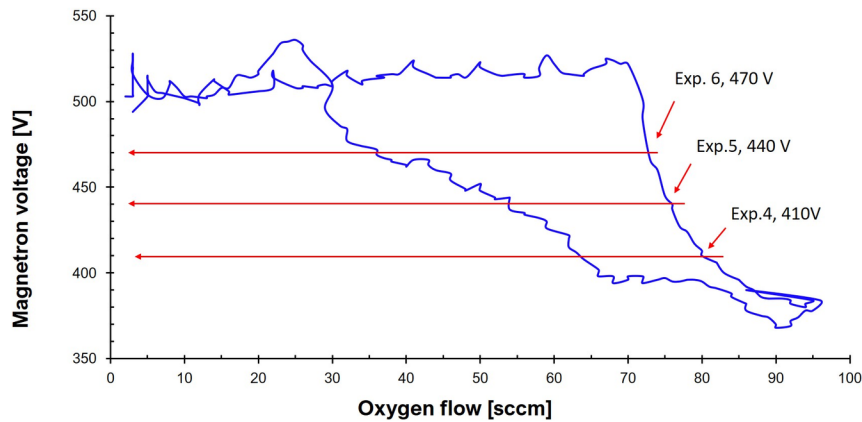


**Figure 4:** Hysteresis characteristics at constant argon flow 160 ml/min

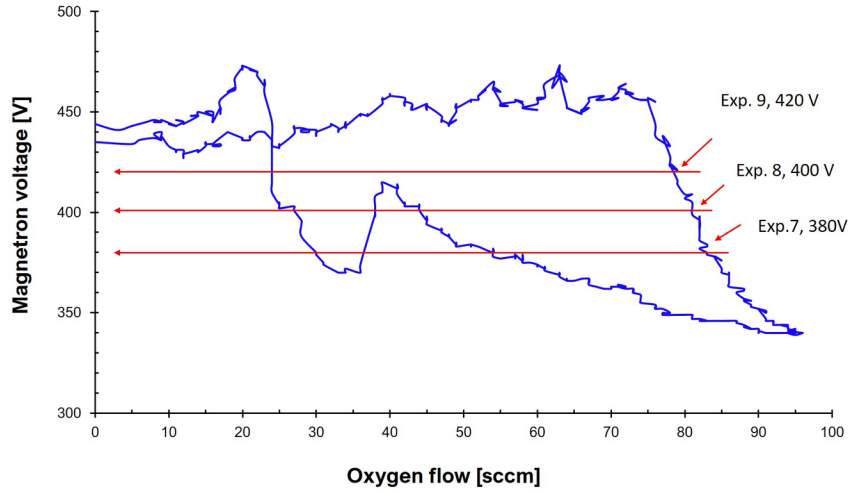


**Figure 5:** Hysteresis characteristics at constant argon flow 200 ml/min

### 3.3 Results

The most important process parameters of the nine coating experiments are summarized in Table 3, whereby the oxygen control range presents the limits of regulation to maintain the specified magnetron voltage. During the coating process, over the duration of five hours, the real magnetron voltage was controlled to the specified magnetron voltage with the oxygen control loop, which was able to maintain the operating points very closely, and thus the absolute process pressure remained constant over the entire coating period. The maximum substrate temperature was measured with a drag indicator thermometer, whereby the lowest substrate temperature measured is 110 °C and the highest substrate temperature is 220 °C. Furthermore, the lowest settled oxygen ratio is 13 % and the highest is 33 %. The scanning electron microscopy images of the fracture surfaces of coating experiments No. 1 to No. 9 were captured using a Zeiss DSM 982 scanning electron microscope. The coated slides were broken in such a way as to crack the coating under tensile load so that the layer structure of the coating thus becomes visible.

**Table 3:** Overview of main process variables in sputtering process

Exp. [No.]	Argon [sccm]	Operating Point [V]	Operating Point Range [V]	Oxygen Control Range [sccm]
1	120	480	470 - 485	52 - 60
2		500	496 - 502	48 - 53
3		520	509 - 523	35 - 45
4	160	410	405 - 416	58 - 76
5		440	436 - 445	48 - 57
6		470	465 - 473	39 - 46
7	200	380	373 - 388	38 - 55

Exp. [No.]	Argon [sccm]	Operating Point [V]	Operating Point Range [V]	Oxygen Control Range [sccm]
8		400	390 - 407	35 - 51
9		420	416 - 425	30 - 44

Figure 6 shows the SEM image of coating No. 6 in which a columnar layer structure is observed for all coatings. The thin titanium adhesion layer, with an average layer thickness of 0.2  $\mu\text{m}$ , has a defect-free interface to the substrate material in all coating experiments. The layer structures of the titanium dioxide coatings are consistently homogeneous, free of defects, and display feature defect-free bonding to the adhesive layer while there is no significant change in the layer structure between coating experiments No. 1 to No. 9.

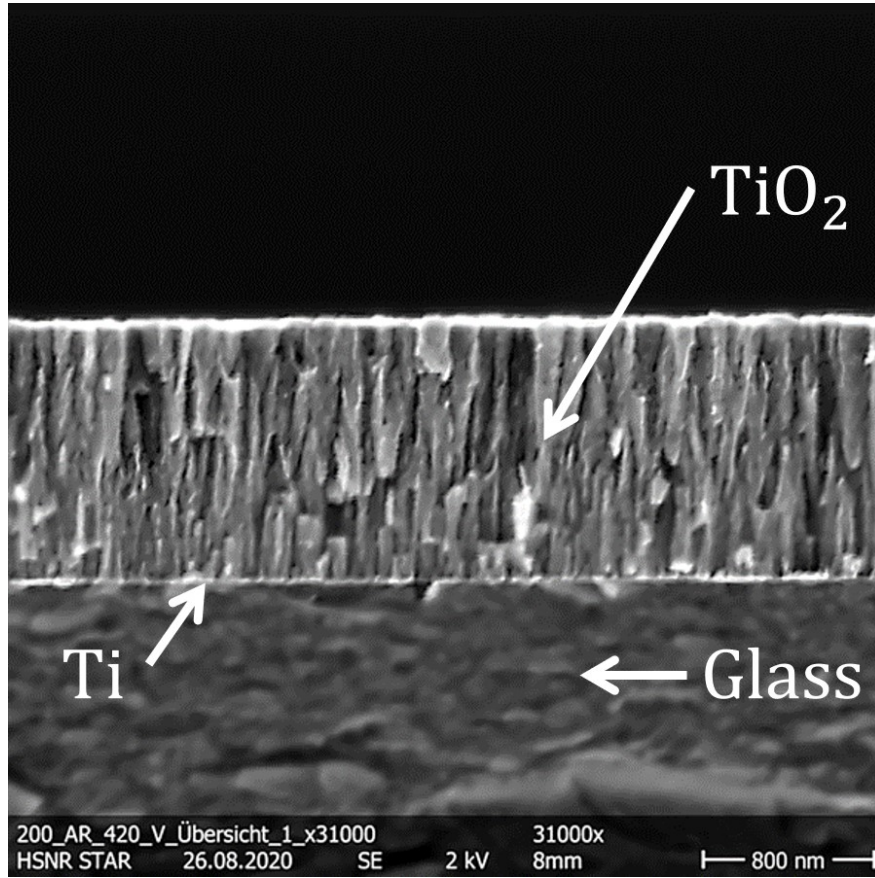
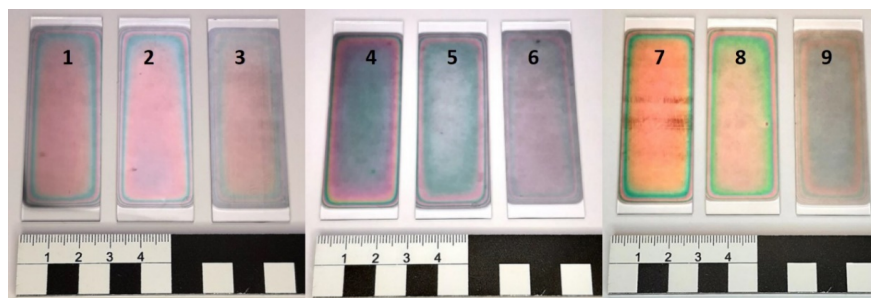


Figure 1:

**Figure 6:** Scanning electron image of a surface break of titanium dioxide 1.0  $\mu\text{m}$  on slide glass (coating experiment No. 9)

Figure 7 shows an image of the coated slide specimens. Figure 8 shows the Raman spectra of the coating experiments No. 1 to No. 3, Figure 9 presents the findings of experiments No. 4 to No. 6, and Figure 10 shows the results of experiments No. 7 to No. 9. The wavenumbers found in all coatings correspond to the anatase phase.



**Figure 7:** Image of  $\text{TiO}_2$  anatase coatings on glass slide from left Experiment No. 1 to right Experiment No. 9

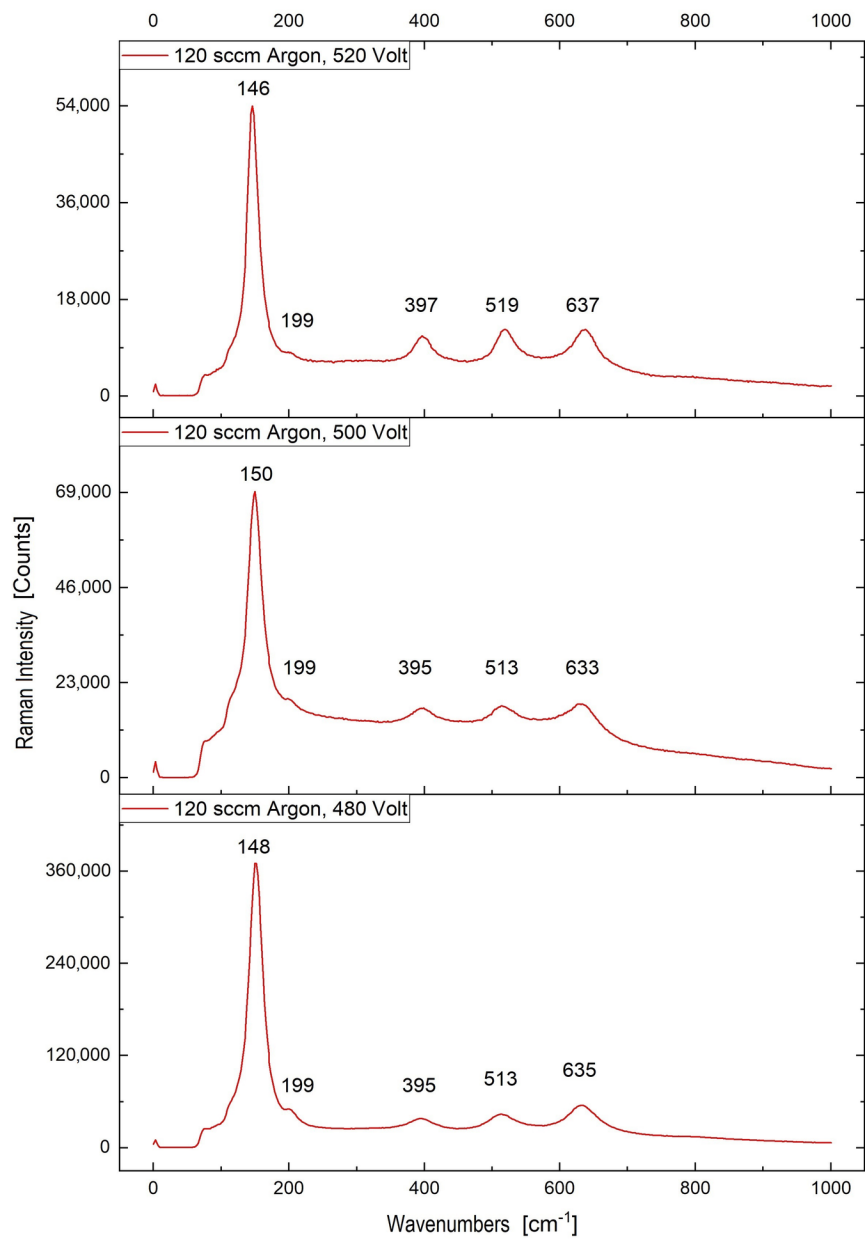


**Figure 8:** Raman spectrum, coating experiments No. 1 (bottom), No. 2 (middle) and No. 3 (top)

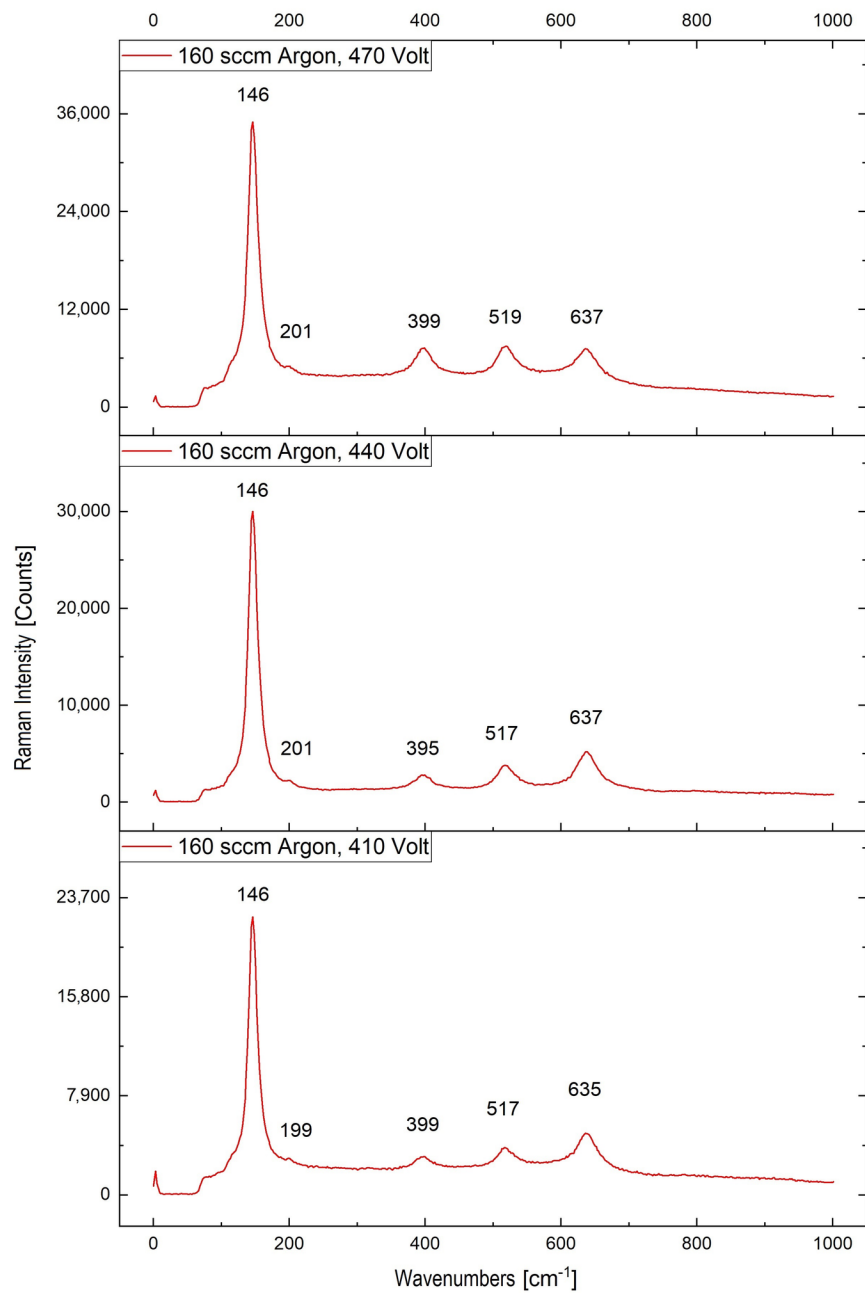


**Figure 9:** Raman spectrum, coating experiments No. 4 (bottom), No. 5 (middle) and No. 6 (top)

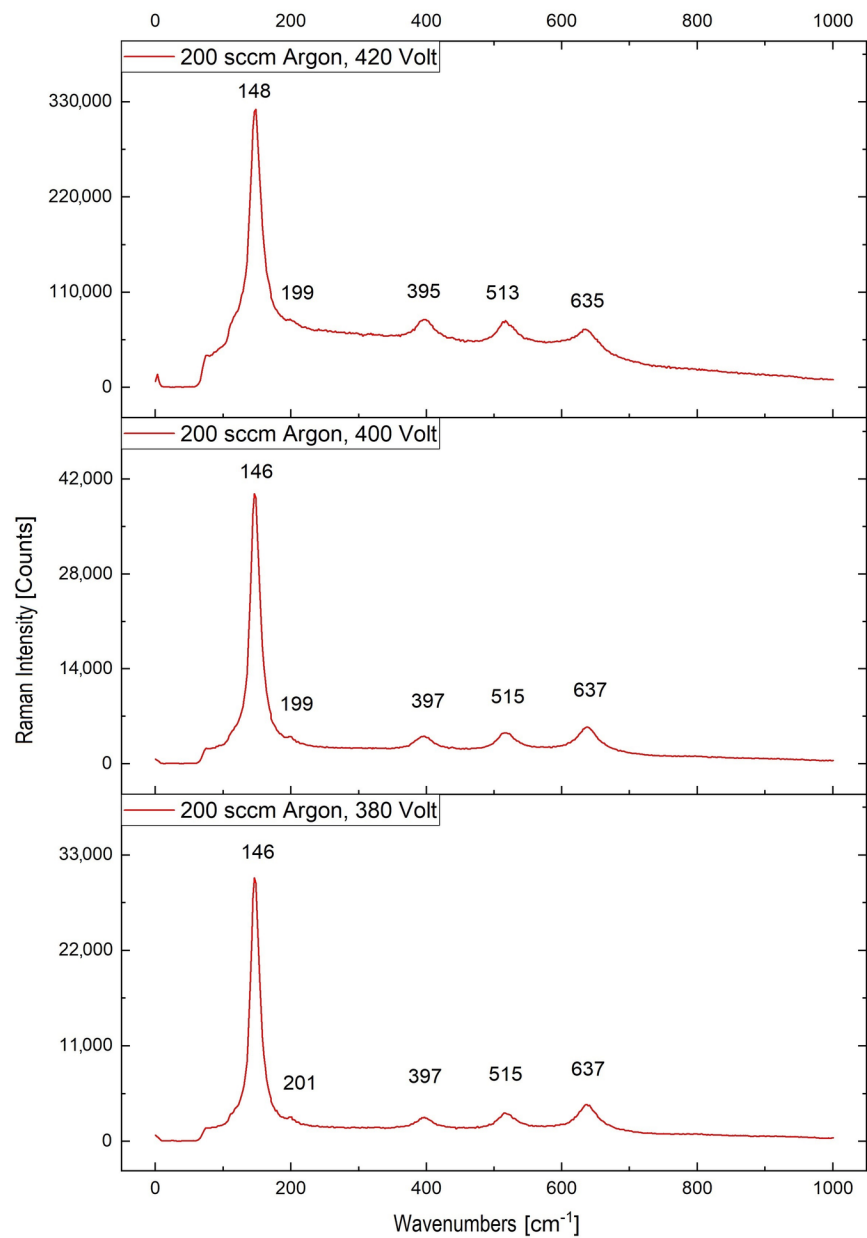


**Figure 10:** Raman spectrum, coating experiments No. 7 (bottom), No. 8 (middle) and No. 9 (top)

## 4. Conclusion

In this work, pulsed DC magnetron sputtering was used for the reactive deposition of titanium dioxide in the anatase phase. The pure anatase phase was detected by Raman spectroscopy on all prepared coatings, whereby the maximum substrate temperature was 220 °C and the lowest substrate temperature was measured in coating experiment No. 9 and amounts to 110 °C. Over a wide process window covering nine coating experiments, the coating remained in the pure anatase phase.

The layer thickness was determined using the calotte grinding method. For evaluation, five coating thickness measurements were averaged in each case and the deviation of the coating thickness measurement was between 0.01  $\mu\text{m}$  and 0.10  $\mu\text{m}$ . The lowest coating thickness was observed in Experiment No. 4 and measures 0.5  $\mu\text{m}$ . Experiment No. 9 has the highest measured film thickness with 1.2  $\mu\text{m}$  while Experiment No. 1 has a film thickness of 0.7  $\mu\text{m}$ , followed by No. 2 at 0.8  $\mu\text{m}$ , No. 3 at 1.1  $\mu\text{m}$ , No. 5 at 0.8  $\mu\text{m}$ , No. 6 at 1.0  $\mu\text{m}$ , and No. 7 and No. 8 display a film thickness of 0.6  $\mu\text{m}$ .

The design of the ideal proportion of oxygen in the oxygen/argon gas mixture reported in the literature for the deposition of the anatase phase during the reactive deposition of titanium dioxide, which is described as ranging from 14.6 % [20] to 34.4 % [23], was indirectly determined in this work by establishing the operating points in the hysteresis experiment. In the coating tests No. 1 to No. 9, the ratio was measured at a minimum of 13 % (coating test No. 9) and a maximum of 33 % (coating test No. 1). The main influencing factor of absolute process pressure, as described in the comparison of coating parameters in the literature from Table 1, was interpreted by attempting to determine the process pressures (Table 2). According to the evaluation of the real process pressure experiment, the pressure ranged between a minimum of  $6.0 \times 10^{-1}$  Pa (coating test No. 3) and a maximum of 2.0 Pa (coating test No. 7). Thus, the range of absolute process pressure of this work is within the promising absolute process pressure of a minimum of  $2.7 \times 10^{-1}$  Pa to 4.0 Pa summarized from the literature as shown in Table 1. The promising absolute process pressure for the deposition of titanium dioxide in the anatase phase according to Table 1 was confirmed using Raman spectroscopic investigations.

The Raman spectroscopic studies show that the pure anatase phase of titanium dioxide is present in all coatings. Five wavenumbers specific to the anatase phase were found in the coating tests No. 1 to No. 9. The characteristic wavenumbers found correspond – with minor deviations – to the six specific wavenumbers of anatase, namely 144  $\text{cm}^{-1}$ , 197  $\text{cm}^{-1}$ , 399  $\text{cm}^{-1}$ , 513  $\text{cm}^{-1}$ , 519  $\text{cm}^{-1}$ , and 639  $\text{cm}^{-1}$  according to the calculations and observations of [26], whereby the two wavenumbers 513  $\text{cm}^{-1}$  and 519  $\text{cm}^{-1}$  are so close to each other that they overlap. The specific wavenumbers were found to be temperature-dependent [27]. Furthermore, different wavelengths of the laser used can lead to a slight deviation in the wavenumber.

The scanning electron microscopic observation of the coatings showed a columnar and homogeneous layer structure in all coating tests, whereby the columnar layer structure was favored due to the relatively low temperature of a maximum of 220  $^{\circ}\text{C}$ , the deposition pressure of minimum  $6.0 \times 10^{-1}$  Pa, and the non-use of an additional BIAS voltage.

## Conflict of Interest Statement

The authors declare no conflict of interest.

## Data availability statement

The data that support the findings of this study are available from the corresponding author upon reasonable request

## References

- 1 W. Baumann and B. Herberg-Liedtke (1996) *Chemikalien in der Metallbearbeitung: Daten und Fakten zum Umweltschutz*, Springer Berlin Heidelberg.
- 2 Kaur, R. and Liu, S. (2016) Antibacterial surface design – Contact kill. *Progress in Surface Science*, **91** (3), 136–153.
- 3 Cassini, A., Liselotte Diaz Högberg, et. al. (2019) Attributable deaths and disability-adjusted life-years caused by infections with antibiotic-resistant bacteria in the EU and the European Economic Area in 2015: a population-level modelling analysis. *The Lancet Infectious Diseases*, **19** (1), 56–66.
- 4 Gastmeier, P., Stamm-Balderjahn, S., Hansen, S., Zuschneid, I., Sohr, D., Behnke, M., Vonberg, R.-P., Rüden, H. (2006) Where should one search when confronted with outbreaks of nosocomial infection? *American journal of infection control*, **34** (9), 603–605.
- 5 Voigt, M. (2017) Photoinduzierte Degradation pharmazeutisch relevanter Substanzen in Wässern - Kinetische, strukturchemische und ökotoxikologische Untersuchungen von Wirkstoffen und deren Abbauprodukten unter Anwendung von Advanced Oxidation Processes. Universität Duisburg-Essen.
- 6 Ren, Y., Han, Y., Li, Z., Liu, X., Zhu, S., Liang, Y., Yeung, K.W.K., Wu, S. (2020) Ce and Er Co-doped TiO<sub>2</sub> for rapid bacteria- killing using visible light. *Bioactive materials*, **5** (2), 201–209.
- 7 Garrido-Cardenas, J.A., Esteban-García, B., Agüera, A., Sánchez-Pérez, J.A., Manzano-Agugliaro, F. (2019) Wastewater Treatment by Advanced Oxidation Process and Their Worldwide Research Trends. *International journal of environmental research and public health*, **17** (1).
- 8 Seyfert, U., Heisig, U., Teschner, G., Strümpfel, J. (2015) 40 Jahre industrielles Magnetron-Sputtern in Europa. *Vakuum in Forschung und Praxis*, **27** (6), 21–26.
- 9 Lake, M. (2009). In: Erich Wintermantel, Suk-Woo Ha. (eds) *Medizintechnik. PVD-Beschichtungstechnologie*, Springer, Berlin, Heidelberg.
- 10 Erkens, G. (2010) *Plasmagestützte Oberflächenbeschichtung: Verfahren, Anlagen, Prozesse und Anwendungen*, Verl. Moderne Industrie, Landsberg/Lech.
- 11 Frey, H. and Khan, H.R. (eds) (2015) *Handbook of thin-film technology*, Springer, Berlin, Heidelberg.
- 12 Energy, A. AE Pulsed DC Products: Precision Process Control | Advanced Energy. <https://www.advancedenergy.com/globalassets/resources-root/brochures/en-ppg-the-pulsed-dc-advantage-brochure.pdf> (14 March 2023).
- 13 Belkind, A., Freilich, A., Lopez, J., Zhao, Z., Zhu, W., Becker, K. (2005) Characterization of pulsed dc magnetron sputtering plasmas. *New J. Phys.*, **7**, 90.
- 14 A. Belkind, Z. Zhao, D. Carter, L. Mahoney, G. McDonough, G. Roche, R. Scholl and H. Walde (2000) *Pulsed-DC Reactive Sputtering of Dielectrics: Pulsing Parameter Effects, 43rd Annual Technical Conference Proceedings—Denver, April 15–20, 2000: Society of Vacuum Coaters 505/856-7188 ISSN 0737-5921*.
- 15 Jürgen Müller (2019) *Presentation: Sputtern Grundlagen: Metaplas PVD Systeme, Grundlagen der Sputtertechnologie, Regelungssysteme für die Abscheidung von Oxiden*, Krefeld.
- 16 J. Sicha, J. Musil, M. Meissner, R. Cerstvý (2008) Nanostructure of photocatalytic TiO<sub>2</sub> films sputtered at temperatures below 200 8C. *Applied Surface Science*, **254**, 3793–3800.
- 17 P. Zeman and S. Takabayashi (2002) Effect of total and oxygen partial pressures on structure of photocatalytic TiO films sputtered on unheated substrate 2. *Surface and Coatings Technology*, **153** (1), 93–99.

- 18 Guillén, C. and Herrero, J. (2017) TiO<sub>2</sub> coatings obtained by reactive sputtering at room temperature: Physical properties as a function of the sputtering pressure and film thickness. *Thin Solid Films*, **636**, 193–199.
- 19 Sarma, B.K., Pal, A.R., Bailung, H., Chutia, J. (2013) Growth of nanocrystalline TiO<sub>2</sub> thin films and crystal anisotropy of anatase phase deposited by direct current reactive magnetron sputtering. *Materials Chemistry and Physics*, **139** (2-3), 979–987.
- 20 P. Löbl, M. Huppertz, D. Mergel (1994) Nucleation and growth in TiO<sub>2</sub> films prepared by sputtering and evaporation. *Thin Solid Films*, **251** (1), 72–79.
- 21 Barnes, M.C., Kumar, S., Green, L., Hwang, N.-M., Gerson, A.R. (2005) The mechanism of low temperature deposition of crystalline anatase by reactive DC magnetron sputtering. *Surface and Coatings Technology*, **190** (2-3), 321–330.
- 22 Toku, H., Pessoa, R.S., Maciel, H.S., Massi, M., Mengui, U.A. (2008) The effect of oxygen concentration on the low temperature deposition of TiO<sub>2</sub> thin films. *Surface and Coatings Technology*, **202** (10), 2126–2131.
- 23 Ratova, M., Klaysri, R., Praserttham, P., Kelly, P.J. (2017) Pulsed DC magnetron sputtering deposition of crystalline photocatalytic titania coatings at elevated process pressures. *Materials Science in Semiconductor Processing*, **71**, 188–196.
- 24 Davisdóttir, S., Shabadi, R., Galca, A.C., Andersen, I.H., Dirscherl, K., Ambat, R. (2014) Investigation of DC magnetron-sputtered TiO<sub>2</sub> coatings: Effect of coating thickness, structure, and morphology on photocatalytic activity. *Applied Surface Science*, **313**, 677–686.
- 25 Varnagiris, S., Urbonavicius, M., Tuckute, S., Lelis, M., Milcius, D. (2017) Development of photocatalytically active TiO<sub>2</sub> thin films on expanded polystyrene foam using magnetron sputtering. *Vacuum*, **143**, 28–35.
- 26 T. Ohsaka, F. Izumi, Y. Fujiki (1978) Raman spectrum of anatase, TiO<sub>2</sub>. *JOURNAL OF RAMAN SPECTROSCOPY*, **7** (6), 321–324.
- 27 T. Ohsaka (1980) Temperature Dependence of the Raman Spectrum in Anatase TiO<sub>2</sub>. *Journal of the Physical Society of Japan*, **48** (5), 1661–1668.